Neuron
Article

p75^{NTR} Mediates Ephrin-A Reverse Signaling Required for Axon Repulsion and Mapping

Yoo-Shick Lim,[1,3] Todd McLaughlin,[1,3] Tsung-Chang Sung,[2,3] Alicia Santiago,[1] Kuo-Fen Lee,[2] and Dennis D.M. O'Leary[1,*]
[1]Molecular Neurobiology Laboratory
[2]Clayton Foundation Laboratories for Peptide Biology
The Salk Institute, 10010 North Torrey Pines Road, La Jolla, CA 92037, USA
[3]These authors contributed equally to this work
*Correspondence: doleary@salk.edu
DOI 10.1016/j.neuron.2008.07.032

SUMMARY

Reverse signaling by ephrin-As upon binding EphAs controls axon guidance and mapping. Ephrin-As are GPI-anchored to the membrane, requiring that they complex with transmembrane proteins that transduce their signals. We show that the p75 neurotrophin receptor (NTR) serves this role in retinal axons. p75^{NTR} and ephrin-A colocalize within caveolae along retinal axons and form a complex required for Fyn phosphorylation upon binding EphAs, activating a signaling pathway leading to cytoskeletal changes. In vitro, retinal axon repulsion to EphAs by ephrin-A reverse signaling requires p75^{NTR}, but repulsion to ephrin-As by EphA forward signaling does not. Constitutive and retina-specific p75^{NTR} knockout mice have aberrant anterior shifts in retinal axon terminations in superior colliculus, consistent with diminished repellent activity mediated by graded ephrin-A reverse signaling induced by graded collicular EphAs. We conclude that p75^{NTR} is a signaling partner for ephrin-As and the ephrin-A- p75^{NTR} complex reverse signals to mediate axon repulsion required for guidance and mapping.

INTRODUCTION

Axonal connections in the mature nervous system are extraordinarily precise. To develop this precision, axons respond to a complex environment of guidance cues as they pathfind and, once within their target, to form an orderly set of connections termed a topographic map. Diverse protein families affect axon pathfinding and mapping, including but not limited to semaphorins, Wnts, neurotrophins, ephrins, and their cognate receptors (Tessier-Lavigne and Goodman, 1996; Huber et al., 2003; McLaughlin and O'Leary, 2005; Flanagan, 2006). In addition, signaling from diverse families of guidance molecules must converge to provide coherent guidance information. Though axon guidance systems eventually link to the cytoskeleton, distinct families of guidance molecules and receptors likely interact at multiple points in their signaling pathways, from ligand binding to intramembrane interactions to cytoskeletal alterations (Grunwald and Klein, 2002; Kullander and Klein, 2002; Murai and Pasquale, 2003).

Here, we use the developing mouse visual system to address the potential for unique interactions between distinct families of potential axon guidance molecules at the origin of signaling events: the axon membrane. Specifically, we examine interactions between the Eph/ephrin families, which have prominent roles in map development (McLaughlin and O'Leary, 2005; Flanagan, 2006), and the p75 neurotrophin receptor (p75^{NTR}; hereafter referred to as p75), a transmembrane protein known for its role in activating signaling pathways for apoptosis and cell survival by differentially interacting with the Trk family of NTRs and neurotrophins (Chao, 2003; Huang and Reichardt, 2003; Barker, 2004).

Eph receptor tyrosine kinases and their ligands, the ephrins, are prominent axon guidance molecules. Ephs and ephrins are each separated into A and B subclasses that exhibit promiscuous receptor-ligand binding and activation within each subclass, but little between subclasses (Gale et al., 1996). All Eph receptors, as well as ephrin-Bs, are transmembrane proteins, whereas ephrin-As are GPI-linked to the cell membrane. In addition, EphB-ephrin-B binding can result in bidirectional signaling, characterized by not only "forward" signaling into cells that express EphBs but also "reverse" signaling into ephrin-B-expressing cells. Reverse signaling by ephrin-Bs is accomplished by association of the intracellular domain of ephrin-Bs with intracellular kinases and phosphatases (Cowan and Henkemeyer, 2002; Kullander and Klein, 2002). EphAs and ephrin-As can also transduce signals bidirectionally, indicating that ephrin-As reverse signal even though they lack an intracellular domain (Davy et al., 1999; Davy and Robbins, 2000; Huai and Drescher, 2001). Reverse signaling by ephrin-As has been implicated in the pathfinding of vomeronasal (Knoll et al., 2001) and spinal motor axons (Marquardt et al., 2005) and the topographic mapping of the axons of olfactory neurons (Cutforth et al., 2003) and retinal ganglion cells (RGCs; Rashid et al., 2005).

Because ephrin-As are anchored to the cell membrane by a GPI linkage and lack an intracellular domain, to reverse signal they must associate with transmembrane proteins capable of activating intracellular signaling pathways. Examples of such associations between GPI-anchored proteins and transmembrane signaling partners in neurons include the transmembrane protein

CASPR and the GPI-linked cell adhesion molecule contactin (Peles et al., 1997) and binding of GDNF to the receptor complex formed by the GPI-anchored receptor GFRα1 and the transmembrane protein c-Ret (Jing et al., 1996; Trupp et al., 1998). However, a transmembrane signaling partner for ephrin-As has not been reported.

As a model for ephrin-A reverse signaling, we have studied the guidance of RGC axons and their formation of a topographic map in the superior colliculus (SC). Ephrin-As are localized to microdomains in the membrane, termed caveolae, which serve as platforms to localize signal transduction by selectively concentrating proteins and facilitating assembly of signaling complexes (Davy et al., 1999; Simons and Toomre, 2000). An enhanced phosphorylation of the Src-family kinase, Fyn, enriched in caveolae has been implicated in ephrin-A reverse signaling and concomitant changes in cytoskeletal architecture to affect cell adhesion (Davy et al., 1999; Davy and Robbins, 2000). Similar to ephrin-As, p75 also localizes to caveolae (Higuchi et al., 2003) and is expressed by RGCs during the developmental period of RGC axon guidance and mapping (Harada et al., 2006). Thus, p75 is a candidate to complex with ephrin-As and initiate their reverse signaling.

The temporal-nasal (T)-(N) axis of the retina maps along the anterior-posterior (A)-(P) axis of the SC. During development, RGC axons differentially respond in a manner relating to their origin along the TN retinal axis to opposing gradients of repellent activities along the AP axis of the SC, resulting in their retinotopic mapping (Yates et al., 2004). The low-to-high AP gradient of repellent activity is due to EphA forward signaling, controlled by a high-to-low TN gradient of EphA receptors on RGC axons and a low-to-high AP gradient of ephrin-As in the SC (reviewed in McLaughlin and O'Leary, 2005; Flanagan, 2006). Computational modeling indicates that, in addition to this low-to-high AP gradient of repellent activity, retinotopic mapping requires an opposing high-to-low AP gradient of repellent activity (Yates et al., 2004). Recent studies in mice have shown that the opposing gradient of repellent activity is due to ephrin-A reverse signaling controlled by a high-to-low NT gradient of ephrin-As on RGC axons and a high-to-low AP gradient of EphAs in the SC (Rashid et al., 2005). Among the findings showing this role for ephrin-A reverse signaling are that RGC axons avoid substrates containing EphA7 in vitro and that genetic deletion of EphA7, which is expressed in a high-to-low AP gradient in the SC but is not expressed in retina, results in aberrant retinocollicular mapping (Rashid et al., 2005).

We hypothesize that ephrin-As and p75 associate in caveolae along RGC axons and that p75 transduces the ephrin-A reverse signal that repels RGC axons and is required for proper AP mapping in the SC. Supporting this hypothesis, we show that p75, ephrin-As, and EphAs are expressed in appropriate patterns by RGCs and in the SC, that p75 colocalizes with ephrin-As in caveolae along RGC axons, and that ephrin-As and p75 form a complex. Further, we show that p75 is required for EphA7 to induce a significant increase in the phosphorylation of Fyn in caveolae, indicating that the Fyn signaling pathway associated with ephrin-A reverse signaling is p75 dependent. In vitro guidance assays show that p75 is required for retinal axons to be repelled by EphAs. In addition, we show, using constitutive and conditional p75 knockout mice, that RGC axons deficient for p75 aberrantly map anterior to their correct targets, as predicted for a diminished repellent effect of ephrin-A reverse signaling. We conclude that p75 acts as a signaling partner with ephrin-As to mediate the repellent effect of ephrin-A reverse signaling on RGC axons upon binding EphAs and that this signaling is required for appropriate retinotopic mapping.

RESULTS

Distributions of EphAs, Ephrin-As, and p75 in Developing Retinocollicular Projection

Previous reports have demonstrated the expression of ephrin-As in gradients in the embryonic and postnatal retina (McLaughlin and O'Leary, 2005). In addition, multiple EphAs are expressed in gradients in the SC (Rashid et al., 2005). For the purpose of our study, we analyzed protein distribution of ephrin-As in the retina and EphAs in the SC at P2, the midpoint in development of retinotopic map in the SC. Immunostaining for ephrin-A5 and ephrin-A2 reveals that each is expressed in a high-to-low NT gradient in the retina, including by RGCs (Figures 1A and 1B). The gradient of ephrin-A5 is steep and restricted primarily to nasal retina, whereas the ephrin-A2 gradient is shallow but extends across most of the NT retinal axis. In addition, both ephrin-A5 and ephrin-A2 are present along RGC axons as they exit the retina and form the optic nerve (Figure 1A and data not shown).

To determine the distribution of EphA protein in the SC at P2, we used an ephrin-A5-Fc affinity probe that binds to all EphAs and is detected by Fc-specific antibodies (Figure 1C). We find that EphAs are distributed in an overall high-to-low AP gradient in superficial layers of the SC where RGC axons navigate across the AP axis of the SC as well as arborize.

p75 is expressed by RGCs throughout development of the retinocollicular projection (Harada et al., 2006). By specific immunostaining, we find that at P2 p75 protein is distributed across the retina with no obvious gradient and is present in RGCs and along RGC axons (Figures 1D and 1E). We find similar distributions of p75 protein at E16, when the first RGC axons reach the SC, through at least P8, when the retinocollicular map resembles its mature form (data not shown). Thus, p75 is distributed along RGC axons at the appropriate time to mediate ephrin-A reverse signaling during their guidance and mapping.

To investigate colocalization of p75 and ephrin-A proteins along RGC axons, we performed immunohistochemistry on primary cultures of dissociated mouse retina. A punctate distribution of both p75 and ephrin-A5 in microdomains that resemble caveolae is found along the primary axon shaft, branches, and growth cones of RGCs (Figures 1F and 1F′). Domains of p75 often colocalize with domains of ephrin-A5 and ephrin-A2, though nonoverlapping domains are also evident (Figure 1F″; data not shown). This colocalization of p75 and ephrin-As in caveolae-like domains along RGC axons is consistent with the distribution required for their biochemical association.

p75 Associates with Ephrin-As and Is Required for Their Reverse Signaling

To establish whether p75 and ephrin-As associate in protein complexes, we carried out a series of immunoprecipitation

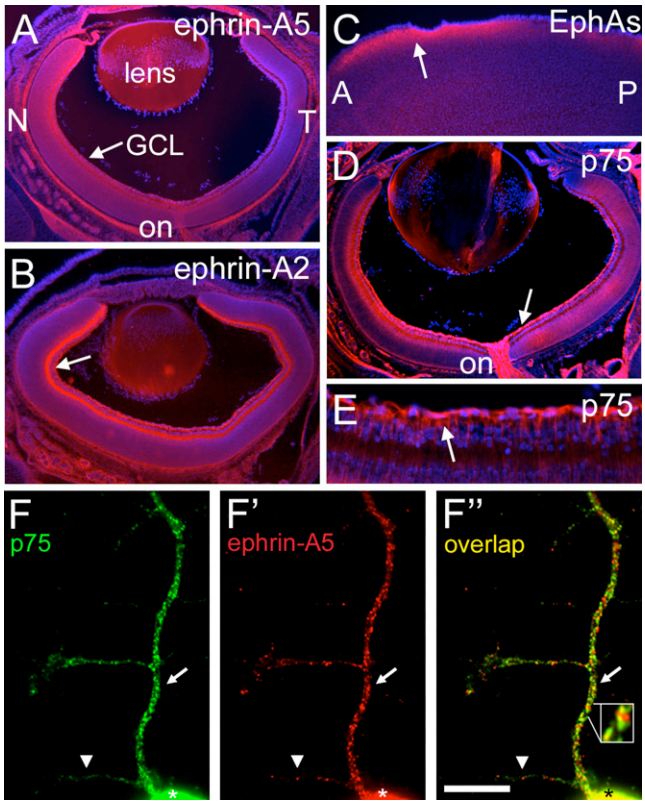

Figure 1. Retinal Expression and Colocalization of p75 and Ephrin-As

(A–E) Cryosections at 20 μm of P2 wild-type mouse stained with DAPI to label nuclei (blue). (A and B) Retina immunolabeled with (A) anti-ephrin-A5 (red) and (B) anti-ephrin-A2 (red). Ephrin-A5 and ephrin-A2 are present in the ganglion cell layer (GCL; arrows), retinal ganglion cells (RGCs), RGC axons, and the optic nerve (on). Ephrin-A5 and ephrin-A2 are present in a high-to-low nasal (N) to temporal (T) gradient. (C) Sagittal section through superior colliculus (SC) labeled with ephrin-A5-Fc affinity probe. EphAs are in a high-to-low anterior (A) to posterior (P) gradient in superficial layers of SC (arrow; red). (D and E) Retina immunolabeled with anti-p75 shown at low (D) and high (E) magnification. p75 (red) is present throughout retina, including the GCL, RGC axons (arrows), and optic nerve.

(F–F″) Mouse retinal axon in vitro double labeled with (F) anti-p75 and (F′) anti-ephrin-A5. Discrete domains of p75 and ephrin-A5 on the cell body (asterisks) and its processes are evident. (F″) Overlap of p75 (green) and ephrin-A5 (red) labeling demonstrates their colocalization (yellow; arrows), though clear domains of each are visible (arrowhead). Colocalized domains are in close proximity to domains of p75 and ephrin-A5 (inset). Scale bar, 50 μm in (A)–(D), 15 μm in (E), 8 μm in (F)–(F″).

assays. Incubating tissue prepared from mouse retina with antibodies against either p75 or ephrin-A2 results in the coimmunoprecipitation of ephrin-A2 and p75, respectively (Figure 2A). We also analyzed PC12 cells, which endogenously express p75, stably transfected with ephrin-A2 linked to the V5 epitope (V5-ephrin-A2). Immunoprecipitation using an antibody specific for p75 (the "Buster" intracellular domain antibody) pulls down V5-ephrin-A2, and a V5 antibody for the tagged ephrin-A2 pulls down p75 (Figure 2B). We also examined the distributions of ephrin-As and p75 on transfected cells in vitro. In 293 cells transfected with cMyc-tagged p75 or V5-ephrin-A5, EphA7-Fc binds only those cells expressing ephrin-A5, indicating that EphA7 itself does not bind p75 extracellularly (Figure 2C). In addition, we find that ephrin-A5 and p75 are found in discrete caveolae-like puncta on the cell membrane, similar to their distributions along RGC axons. Immunoprecipitations and western blots performed on 293T cells transiently cotransfected with cMyc-p75 and either V5-ephrin-A5 or V5-ephrin-A2 using antibodies directed against either the cMyc or V5 epitopes coimmunoprecipitate p75 with either ephrin-A2 or ephrin-A5 (Figure 2C). Thus, these findings using cell lines corroborate those obtained with mouse retina and together suggest that ephrin-As and p75 are present as a protein complex in the membrane. This association between p75 and ephrin-As, together with their colocalization in discrete domains along RGC axons, suggests functional implications for p75-ephrin-A complexes in activating intracellular signaling, in response to EphAs, that controls RGC axon guidance and mapping.

Fyn has been implicated in ephrin-A reverse signaling (Davy et al., 1999). Therefore, we performed experiments to determine whether p75 is involved in the Fyn signaling pathway associated with ephrin-A reverse signaling. We first established that EphA7-Fc binds ephrin-As but does not bind p75 on the surface of transfected 293 cells (Figure 2C), indicating that EphA7 is not a ligand for p75 but is a ligand for ephrin-A. Although p75 does not bind EphAs, we show below that the association of p75 with ephrin-A is required for ephrin-A reverse signaling.

We next examined the phosphorylation of Fyn in stably transfected 293 cells to determine whether Fyn phosphorylation associated with ephrin-A reverse signaling is dependent upon p75. Previous studies of ephrin-A reverse signaling in transfected cell lines have shown that the enhanced phosphorylation of Fyn occurs predominantly in the caveolae fraction, with a very minor increase in the soluble fraction (Davy et al., 1999). These findings are consistent with the preferential localization of ephrin-As and p75 to caveolae (Davy et al., 1999; Higuchi et al., 2003; present study). Therefore, we focused on caveolae-containing fractions isolated from stably transfected 293 cells and identified with antibodies against the caveolae-specific protein, flotillin-1 (Higuchi et al., 2003; Slaughter et al., 2003), and the presence of the caveolae-specific lipid, GM1 (Parton, 1994; Figure 3). We used EphA7-Fc to stimulate ephrin-A reverse signaling by its binding of ephrin-A, and as a control for this stimulation, we used Fc alone. These are the same proteins that we use in the protein stripe assay, described in the following section, to show that the repellent effect of ephrin-A reverse signaling on retinal axons is dependent upon p75.

We find that in cells stably transfected with either ephrin-A2 or p75, the level of phosphorylated Fyn or even overall phosphotyrosine levels do not change after treatment with EphA7-Fc compared to Fc treatment (Figures 3A and 3B). However, when both ephrin-A2 and p75 are present, we find a significant increase in the overall level of both phosphotyrosine and Fyn after treatment with EphA7-Fc, compared to treatment with Fc, in the caveolae fractions (n = 2; Figure 3C). These data indicate that p75 complexes with ephrin-As and is required for activation of ephrin-A reverse signaling through an intracellular pathway involving Fyn. Interestingly, we also find that the level of p75 is increased

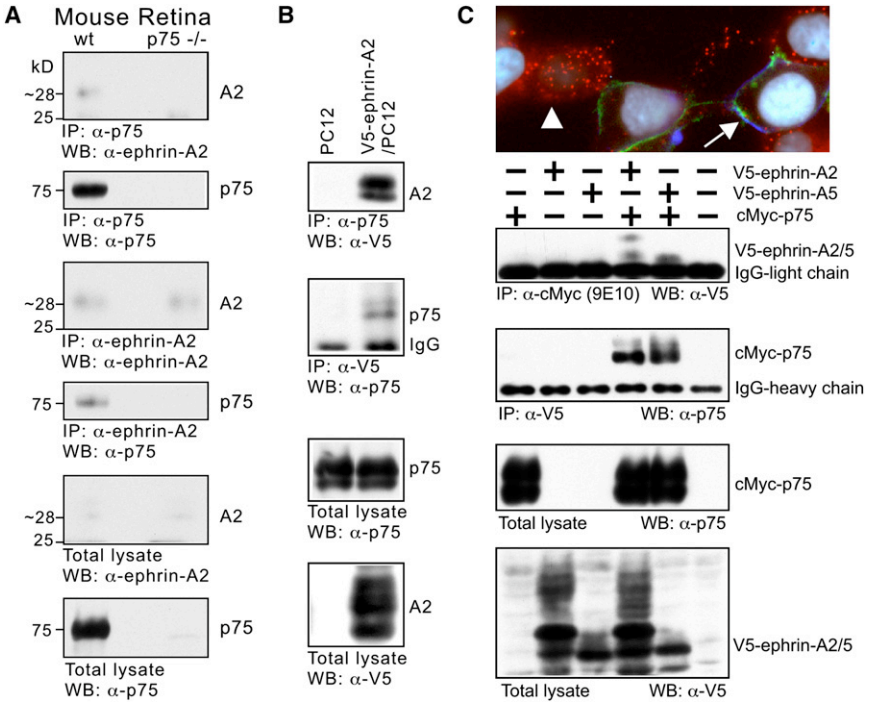

Figure 2. Ephrin-As and p75 Are Present in the Same Complex

(A) Retina from wild-type and p75 null mutant mice immunoprecipitated (IP) with anti-p75 antibody (Buster) or anti-ephrin-A2 antibody (R&D systems). Western blots (WB) reveal that p75 and ephrin-A2 co-IP.

(B) PC12 cells and PC12 cells stably transfected with V5-ephrin-A2 immunoprecipitated with the antibody indicated. Western blots demonstrate that p75 (endogenously expressed by PC12 cells) and V5-ephrin-A2 co-IP.

(C) Triple-immunolabeled 293 cells transfected with V5-ephrin-A2 or cMyc-p75. Cells were incubated with EphA7-Fc and triple labeled with antibodies against cMyc, V5, and Fc. Both p75 (red, arrowhead) and ephrin-A2 (blue) are in a punctate distribution on distinct cells. EphA7-Fc (green, arrow) labels only cells transfected with V5-ephrin-A2. Cells are also stained with DAPI (white; nuclei). Western blots after IPs with the antibodies listed on 293T cells transiently transfected with the construct(s) indicated (+) demonstrate that ephrin-A2 and ephrin-A5 co-IP with p75.

in the caveolae fractions following EphA7-Fc treatment, compared to Fc treatment, in cells in which ephrin-A2 is also present. In addition to the substantial increase in phosphotyrosine level induced by EphA, the findings that the recruitment of p75 and Fyn to caveolae is also dependent on EphA binding ephrin-A supports their involvement in ephrin-A reverse signaling.

Repellent Effect of EphA7 on Retinal Axons Requires p75

We used the protein stripe assay to assess whether the repellent activity of ephrin-A reverse signaling for retinal axons requires their expression of p75. Axons extending from retinal explants from P0 wild-type ($p75^{+/+}$) and p75 knockout mice ($p75^{-/-}$; Lee et al., 1992) were given a choice to grow on alternating stripes of EphA7-Fc and Fc, or in control experiments, alternating stripes that each contain Fc (Figure 4). We chose EphA7 because it is expressed in a high-to-low AP gradient in the SC and repels wild-type retinal axons in the protein stripe assay (Rashid et al., 2005). In control experiments, neither $p75^{+/+}$ nor $p75^{-/-}$ retinal axons exhibit a growth preference for either set of Fc stripes (Figures 4A and 4B). However, when given a choice between alternating stripes of EphA7-Fc and Fc, $p75^{+/+}$ retinal axons demonstrate a strong preference for stripes containing Fc and a strong avoidance of stripes containing EphA7-Fc (Figure 4C). In contrast, $p75^{-/-}$ retinal axons do not exhibit a significant preference for either the EphA7-Fc or Fc set of stripes and

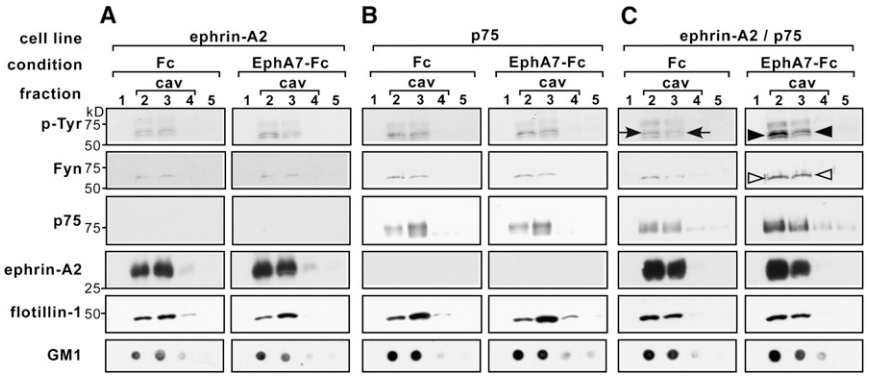

Figure 3. EphA-Induced Fyn Phosphorylation in Caveolae Requires p75

(A–C) Stably transfected V5-ephrin-A2, p75, and V5-ephrinA2/p75 293 cells treated with Human-Fc (2 μg/ml) or EphA7-Fc (2 μg/ml) for 10 min at 37°C. Cells were lysed and fractionated through a sucrose gradient (see Experimental Procedures). The presence of the caveolae (cav) associated protein flotillin-1, detected with an anti-flotillin-1 antibody, and GM1, detected with CTX-HRP in a dot blot, indicates the fractions containing caveolae. Tyrosine phosphorylation (p-Tyr; 4G10 antibody) in the caveolae fractions is unchanged when challenged with EphA7-Fc compared to Fc in both the (A) ephrin-A2 cell line and the (B) p75 cell line. (C) In contrast, the ephrin-A2/p75 cell line has a higher level of p-Tyr in caveolae fractions (arrowheads) when treated with EphA7-Fc compared to Fc alone (arrows). The largest increase in p-Tyr (arrowheads) is coincident with the location of Fyn on the reprobed blot (hollow arrowheads).

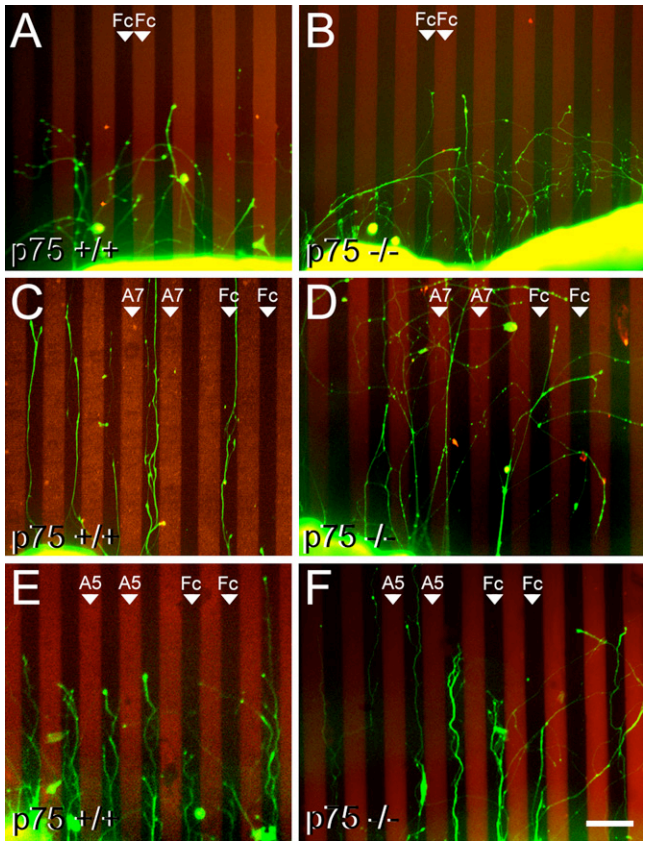

Figure 4. Retinal Axons Require p75 for EphA7 Repulsion

(A–D) In vitro protein stripe assays demonstrating that wild-type RGC axons preferentially avoid stripes containing EphA7 but $p75^{-/-}$ RGC axons do not. (A and B) Axons (green) extending on a control substrate of alternating stripes of human-Fc and human-Fc (Fc). Axons do not show a growth preference for one stripe over the other whether they extend from (A) a $p75^{+/+}$ mouse retinal explant or from (B) a $p75^{-/-}$ retinal explant. (C and D) Axons extending on a substrate of alternating stripes of human-Fc and EphA7-Fc (red; A7). (C) Axons from a $p75^{+/+}$ retinal explant preferentially extend on the human-Fc stripes and avoid the EphA7 stripes. (D) In contrast, axons from a $p75^{-/-}$ retinal explant do not avoid stripes containing EphA7.

(E and F) Axons extending on a substrate of alternating stripes of human-Fc and ephrin-A5-Fc (red; A5). Axons show a strong preference for the Fc-containing stripes and avoid the ephrin-A5-containing stripes whether they extend from (E) a $p75^{+/+}$ retinal explant or from (F) a $p75^{-/-}$ retinal explant. Scale bar, 200 μm.

instead have similar outgrowth on each set (Figure 4D). These qualitative impressions of the growth preferences are supported by three distinct quantitative methods, all performed blind to genotype and stripe content, that include the classic method of scoring growth preference on a scale from 0 to 4 (Figure 5A; Walter et al., 1987), quantification of pixels representative of stained axons on each set of stripes (Figure 5B), and a modified Sholl intersection analysis (Sholl, 1953; Figures 5C and 5D) (see Experimental Procedures for details).

We performed additional stripe assay experiments to assess potential effects of p75 deficiency on the repellent effect of EphA forward signaling in response to ephrin-As exhibited by retinal axons. These experiments were carried out as described above except EphA7-Fc was replaced with ephrin-A5-Fc. We find that $p75^{+/+}$ retinal axons preferentially avoid ephrin-A5-containing stripes (Figure 4E), consistent with previous reports (e.g., Feldheim et al., 1998), and that $p75^{-/-}$ retinal axons also show a strong avoidance of ephrin-A5 stripes (Figure 4F) indistinguishable from wild-type (Figures 5A and 5D). Therefore, $p75^{+/+}$ and $p75^{-/-}$ retinal axons exhibit a similar repellent response to ephrin-A5 mediated by EphA forward signaling.

In additional experiments, we titrated the concentration of ephrin-A5-Fc in the stripes to the level at which $p75^{+/+}$ retinal axons exhibit a small but significant preference for the Fc set of stripes (coefficient of choice = 0.22; $p < 0.05$; n = 9; see Experimental Procedures). We find that matched sets of retinal explants from $p75^{-/-}$ mice grown on the same substrates in the same dish as the retinas from $p75^{+/+}$ littermates exhibit a similar degree of preference for the Fc stripes (coefficient of choice = 0.20; $p < 0.05$; n = 9; coefficients of choice are not significantly different from each other). Thus, $p75^{+/+}$ and $p75^{-/-}$ retinal axons exhibit the same degree of repulsion to ephrin-A5 at both high and low concentrations of the repellent activity. These data indicate that $p75^{-/-}$ retinal axons are not only repelled by ephrin-A5 to a similar degree as $p75^{+/+}$ retinal axons but that both exhibit the same sensitivity to ephrin-A5. Thus, p75 deficiency does not significantly influence EphA forward signaling in retinal axons or mechanisms required for them to exhibit a repellent response.

We also find that $p75^{+/+}$ and $p75^{-/-}$ retinal axons do not exhibit significant differences in general outgrowth. For example, over all of the stripe experiments described, $p75^{+/+}$ retinal explants extend on average 26 axons, similar to $p75^{-/-}$ retinal explants that extend 25 axons (n = 47 for $p75^{+/+}$; n = 37 for $p75^{-/-}$; n.s.). Similarly, the extent of axon growth is similar between genotypes. For example, ~27% of all axons that extend at least 100 μm from a retinal explant also extend 900 μm for both $p75^{+/+}$ and $p75^{-/-}$ retinas (n = 1237 axons for $p75^{+/+}$; n = 933 axons for $p75^{-/-}$; n.s).

We conclude that the lack of avoidance of EphA7-Fc by $p75^{-/-}$ retinal axons is not due to a general inability to extend or respond to guidance cues but rather is due to a specific defect in ephrin-A reverse signaling. Taken together, these data show that p75 mediates the repellent effect of EphAs on retinal axons and together with our biochemical and colocalization data strongly suggest that p75 is a signaling partner for ephrin-A reverse signaling.

Use of p75 Mutant Mice to Study Requirement for p75 in Retinotopic Mapping

Our findings that p75 is required in vitro for the repulsion of retinal axons by ephrin-A reverse signaling suggest that p75 is required for the proper development of the retinotopic map in the SC. We predict that in the absence of p75, repulsion of RGC axons mediated by ephrin-A reverse signaling will be diminished, resulting in an anterior shift of their projections. To address this issue, we used complementary axon tracing methods to analyze the topographic organization of the retinocollicular projection in constitutive p75 knockout mice (Lee et al., 1992) and in conditional p75 knockout mice in which floxed (fl) alleles of p75 were selectively deleted from RGCs localized to specific retinal domains (mouse described in Z. Chen, T.-C. S., N. Harada, W. Lin, and K.-F.L., unpublished data). One labeling method is anterograde labeling of

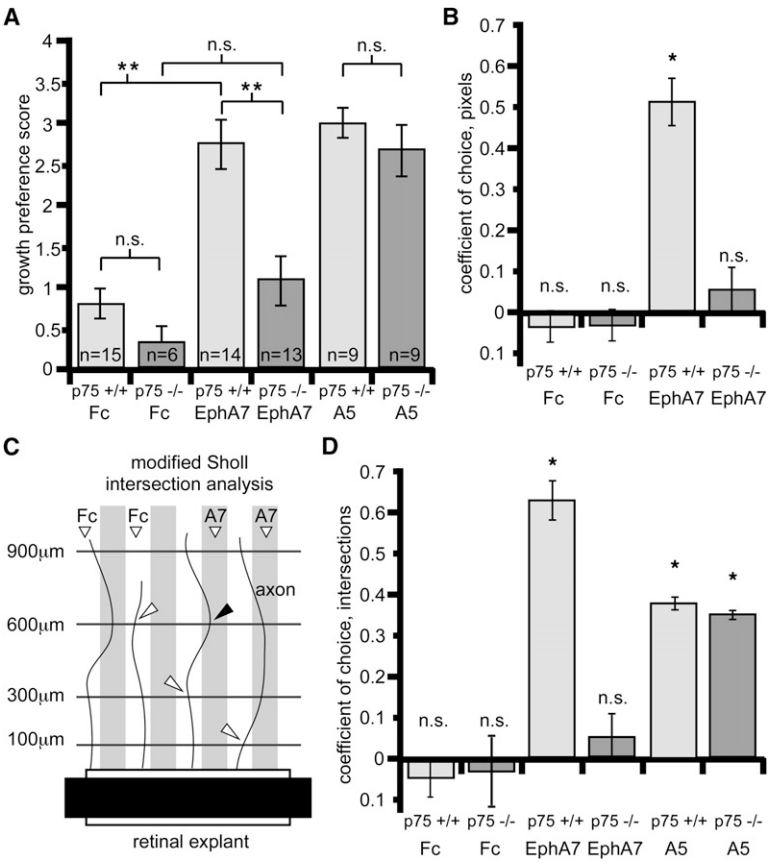

Figure 5. Statistical Analysis of Stripe Assay Results

(A) Average growth preference scores (error bars = SEM) for retinal axons in the stripe assay (see Experimental Procedures). A score of four is an essentially complete choice for one stripe; a score of zero is no discernible choice for either stripe. Retinal axons do not show a preference on control human-Fc versus human-Fc (Fc) substrates. Retinal axons from $p75^{+/+}$ explants show significant avoidance of EphA7 compared to retinal axons from $p75^{-/-}$ explants. In contrast, axons extending from $p75^{+/+}$ or $p75^{-/-}$ explants avoid ephrin-A5 (A5) to a similar extent.

(B) The coefficient of choice for $p75^{+/+}$ and $p75^{-/-}$ axons extending on control Fc versus Fc substrates or EphA7-Fc versus Fc substrates is shown. Pixels representing axons present in each stripe were quantified and the coefficient calculated as the number of pixels on the Fc stripe minus pixels on the second stripe (Fc or EphA7), divided by total pixels (see Experimental Procedures). A coefficient of one is an absolute choice for the control stripe, and a coefficient of zero indicates no preference. $p75^{+/+}$ axons preferentially avoid EphA7 stripes, whereas $p75^{-/-}$ axons do not show a significant preference for Fc stripes compared to EphA7 stripes.

(C and D) Protein stripe assays analyzed with a simplified Sholl intersection analysis. (C) Schematic demonstrates the analysis method (see Experimental Procedures). All intersections (arrowheads) between axons and lines at defined distances from the explant edge were counted blind to genotype, stripe content, and stripe position. (D) Coefficients of choice for intersection points determined by the modified Sholl analysis (intersections on the Fc stripe minus intersections on the second stripe (Fc or EphA7 or ephrin-A5), divided by total intersections). On Fc versus Fc substrates, there is no significant choice for either stripe. In contrast, $p75^{+/+}$ axons extending on Fc versus EphA7 substrates intersect the Sholl lines significantly more often on Fc stripes than on EphA7 stripes. However, in $p75^{-/-}$ axons, this preference is greatly reduced, and the number of intersection points on Fc and EphA7 stripes is not significantly different. For both $p75^{+/+}$ and $p75^{-/-}$ axons extending on Fc versus ephrin-A5 substrates, significantly more intersection points occur on Fc stripes compared to ephrin-A5 stripes. n values in panel (A) apply to panels (B) and (D). n.s., not significant; *$p < 0.02$, **$p < 0.001$.

a small number of RGC axons by a small focal injection of the lipophilic axon tracer DiI in the retina. The other method labels, in a reproducible manner, large domains of RGCs and their axonal terminations using a conditional eGFP marker and the α-cre recombinase allele that is expressed in nasal and temporal retina but not in central retina or along the visual pathway (Marquardt et al., 2001; Baumer et al., 2002; data not shown).

We verified that the development, size, and patterning of the retina are normal in the constitutive and conditional p75 mutants. Markers specific for RGCs (e.g., Brn3.2; Figures 7C and 7C′; Xiang et al., 1993), as well as general cell stains, reveal that at late embryonic and postnatal ages the size and laminar patterning of the retina, and density of RGCs, is indistinguishable between $p75^{-/-}$ mice and their $p75^{+/+}$ littermates (data not shown; also Harada et al., 2006). Further, these genotypes have no difference in the graded expression of ephrin-A2 and ephrin-A5, indicating that expression of axon guidance molecules and axial patterning of the retina is normal in the absence of p75 (data not shown).

Analyses of Constitutive Null p75 Mice

We first analyzed the topographic organization of the retinocollicular projection in constitutive null p75 mice and their $p75^{+/+}$ littermates by making a small focal injection of DiI into peripheral nasal retina. At neonatal stages, prior to map refinement, the projections labeled in $p75^{+/+}$ and $p75^{-/-}$ mice are indistinguishable, including the degree of axon overshoot (data not shown). By P8, when the map is normally properly ordered (Frisen et al., 1998), a nasal DiI injection in $p75^{+/+}$ mice labels a dense, focal TZ in the topographically appropriate position in posterior SC (n = 11; Figure 6A). A similar nasal injection of DiI in $p75^{-/-}$ mice results in a dense, focal TZ, but in every case the TZ is shifted anteriorly compared to its position in $p75^{+/+}$ littermates (n = 8; Figure 6B). Quantification shows that the positions of the DiI injection sites on the TN retinal axis are not statistically different between genotypes, but in contrast the anterior shift of the TZ formed by nasal RGC axons on the AP SC axis in $p75^{-/-}$ mice compared to $p75^{+/+}$ littermates is statistically significant (Figure 9A). Additionally, the AP position of the TZ in each $p75^{-/-}$ case is positioned anterior to the mean TZ position for $p75^{+/+}$ cases (Figure 9B).

In addition to an anterior shift in the TZ in $p75^{-/-}$ mice, in half of the $p75^{-/-}$ cases, ectopic branches and arbors are present along the AP length of nasal axons in the SC at P8 (Figure 6B), an age when the retinotopic map in $p75^{+/+}$ mice is refined to its mature form and branches are not observed outside the TZ.

To study the organization of the retinocollicular map at a population level, the α-cre line, which expresses cre recombinase in

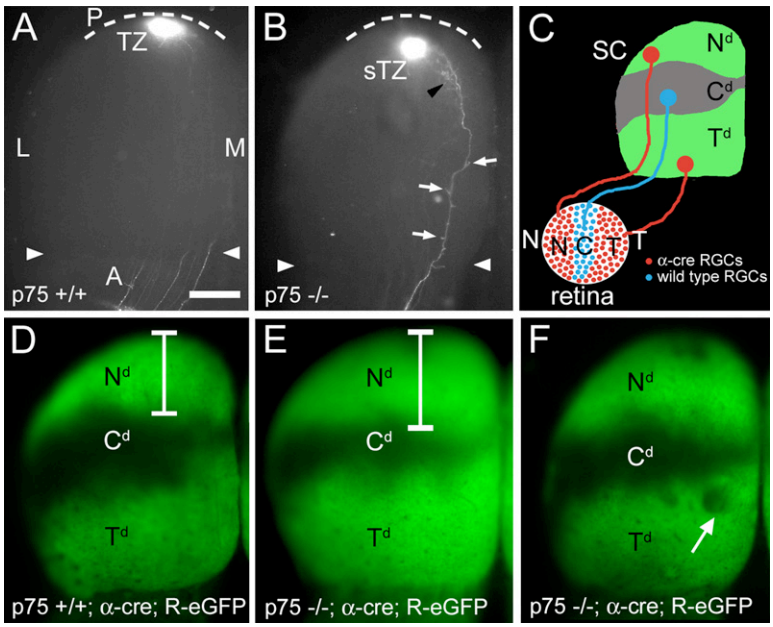

Figure 6. Aberrant Retinocollicular Mapping in p75 Knockout Mice

(A) Dorsal view of the superior colliculus (SC) of a P8 wild-type mouse after focal injection of DiI in nasal (N) retina reveals a dense termination zone (TZ) in posterior (P, dotted line is posterior SC border) SC. No interstitial branches are evident in the SC outside of the TZ at this age in $p75^{+/+}$ mice. Arrowheads mark the anterior (A) border.

(B) SC of a P8 $p75^{-/-}$ mouse injected with DiI in nasal retina (injection is similar in size and location to that in panel [A]) reveals a dense TZ in posterior SC, but shifted anteriorly (sTZ) in comparison to wild-type. Multiple branches (arrows) and rudimentary arbors (black arrowhead) are evident throughout the SC, anterior to the TZ.

(C) Schematic describing the expression of cre-recombinase in nasal and temporal retinal ganglion cells (RGCs; red) in α-cre mice. The α-cre line in combination with the ROSA-GAP43-eGFP (R-eGFP) line results in a stereotypic pattern of eGFP-labeled RGC axons (green) in three distinct domains in the SC, corresponding to the eGFP-labeled projection from temporal (T^d) and nasal (N^d) retina and the unlabeled central domain (C^d).

(D) Dorsal view of the SC of a $p75^{+/+}$; α-cre; R-eGFP mouse illustrating the stereotypic pattern of R-eGFP in wild-type mice. Bracket denotes the anterior-posterior extent of the N^d.

(E and F) RGC projections in $p75^{-/-}$; α-cre; R-eGFP mice show an anterior shift in nasal RGC axon mapping.

(E) Bracket denotes an extended, anteriorly shifted N^d.

(F) In some $p75^{-/-}$ cases, the eGFP is discontinuous and has gaps (arrow), indicating a disorganized projection. These gaps are not observed in $p75^{+/+}$; α-cre; R-eGFP mice. L, lateral; M, medial. Scale bar, 400 μm.

nasal and temporal retina but not in central retina (Marquardt et al., 2001; Baumer et al., 2002), was crossed to the ROSA-GAP43-eGFP line (R-eGFP) that requires cre-mediated deletion of a floxed-stop cassette to express an eGFP reporter under control of the ROSA promoter (Sapir et al., 2004). This strategy selectively labels nasal and temporal retina, including RGC axons and their terminations within the SC (Figure 6C). We crossed this α-cre; R-eGFP compound line with p75 mutant mice to study more broadly the effect of p75 deletion on retinotopic mapping.

In $p75^{+/+}$; α-cre; R-eGFP mice, the projections of RGCs in the nasal and temporal domains of retina are labeled by eGFP, revealing the retinotopic pattern of their terminations, that include a nasal domain (N^d) in posterior SC and a temporal domain (T^d) anterior SC, respectively, as well as an eGFP-negative central domain (C^d) formed by the axonal terminations of RGCs in central retina that do not express cre (n = 10; Figures 6C and 6D). However, in $p75^{-/-}$; α-cre; R-eGFP mice, the N^d of this termination pattern formed by eGFP-positive nasal RGC axons shows a significant anterior expansion into the eGFP-negative C^d formed by eGFP-negative central RGC axons (n = 7; Figures 6E and 6F). Further, in a subset of these $p75^{-/-}$ cases, regions of lower eGFP expression are evident in the T^d (Figure 6F). These regions of diminished eGFP expression are not observed in $p75^{+/+}$ littermates, indicating a level of disorganization in the retinotopic map of $p75^{-/-}$ mice that likely reflects ectopic arborizations formed by eGFP-negative central RGC axons, consistent with DiI labeling in $p75^{-/-}$ mice.

To quantify these mapping changes in p75 mutants, we measured the relative mean areas occupied by each of the three projection domains (N^d, C^d, and T^d) in the SC (Figure 9; see Experimental Procedures). Compared to $p75^{+/+}$ mice, the N^d shows a significant increase in area in the $p75^{-/-}$ mice (13% increase, $p < 0.02$), confirming an anterior shift in the TZs of p75-deficient nasal axons. Consistent with this anterior shift, the C^d is diminished in size in $p75^{-/-}$ mice compared to $p75^{+/+}$ mice (27% decrease, $p < 0.02$). In summary, in $p75^{-/-}$ mice, the terminations of nasal RGC axons in the SC are shifted anteriorly to those in $p75^{+/+}$ mice. The total area of the SC is not significantly different between genotypes (data not shown); thus, these differences in the sizes of the termination domains are both relative and absolute. This anterior shift of the terminations of RGC axons is consistent with a diminished repellent effect of ephrin-A reverse signaling due to their loss of the ephrin-A signaling partner, p75.

Analyses of Mice with Retina-Specific Deletion of Floxed Alleles of p75

To further study the influence of p75 on retinotopic mapping in vivo, we analyzed mice with a conditional allele (floxed, fl) of p75 that can be removed by cre recombinase. For wild-type controls, we used mice containing the p75 floxed allele but not the α-cre allele (p75 fl/fl or p75 fl/+ and cre negative) and $p75^{+/+}$; α-cre; R-eGFP mice, none of which affect retinocollicular development or mapping (data not shown). In $p75^{+/+}$; α-cre; R-eGFP mice, the nasal and temporal retina are labeled by eGFP without affecting p75 expression (Figures 7A and 7A′). In p75 fl/fl; α-cre; R-eGFP mice, eGFP is also expressed in nasal and temporal retina, but p75 protein is also selectively eliminated; cells in central retina lack cre recombinase and therefore do not express eGFP and retain wild-type levels of p75 protein (Figures 7B and 7B′). This altered pattern of p75 protein distribution in p75 fl/fl; α-cre mice is evident prior to E16, when RGC axons first reach the SC, and thereafter.

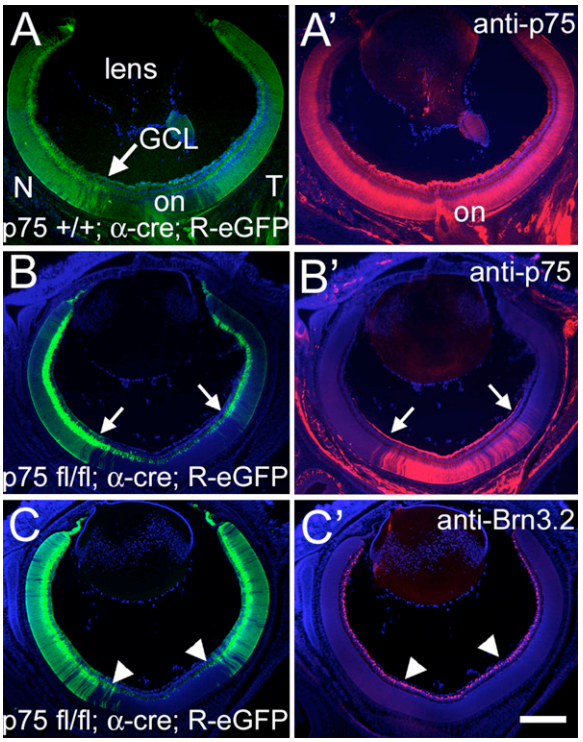

Figure 7. Conditional Allele of p75 Is Excised with Cre Recombinase

(A and A′) Cryosection through a P2 $p75^{+/+}$; α-cre; R-eGFP mouse. The nasal (N) and temporal (T) aspects of the retina, including the ganglion cell layer (GCL), are labeled with eGFP, mimicking cre expression. The distribution of p75 is unaffected in $p75^{+/+}$; α-cre; R-eGFP mice.

(B and B″) However, in p75 fl/fl; α-cre; R-eGFP mice, p75 protein is not detectable at P2 in nasal and temporal retina but is unchanged in central retina. The eGFP label in panel (B) indicates the presence of cre-recombinase and, thus, the cells in which p75 has been excised. The arrows are in the same position and denote the border of eGFP expression.

(C and C′) Cryosection from the retina of a p75 fl/fl; α-cre; R-eGFP mouse labeled for the RGC marker Brn3.2 at P2. The proportion of RGCs in central retina, where p75 expression is unaltered, is identical to that in nasal and temporal retina, where p75 is absent. Arrowheads denote the edges of cre expression. Scale bar, 40 μm.

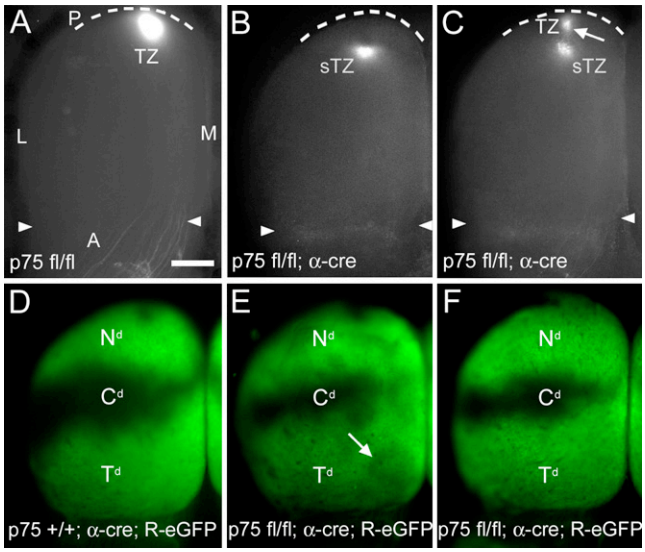

Figure 8. Aberrant Retinocollicular Mapping in p75 Conditional Mice

(A) Dorsal view of the superior colliculus (SC) of p75 fl/fl; cre-negative mouse at P8 after focal injection of DiI in nasal retina reveals a dense termination zone (TZ) in posterior (P) SC (dotted line is posterior SC border; arrowheads mark the anterior [A] SC border).

(B and C) SCs of p75 fl/fl; α-cre mice at P8 after focal injections of DiI in nasal retina, similar in size and location to that in panel (A). (B) In every p75 fl/fl; α-cre case, the TZ is shifted (sTZ) anteriorly compared to its expected position. (C) In a subset of p75 fl/fl; α-cre mice, focal DiI injection reveals two TZs in posterior SC. The arrow points to the appropriate location of the TZ, with an sTZ in an anterior position.

(D) A $p75^{+/+}$; α-cre; R-eGFP case illustrates the stereotypic pattern of the eGFP-labeled temporal and nasal RGC axon projection domains (T^d and N^d, respectively). The projection domain from central retina (C^d) is unlabeled.

(E and F) In p75 fl/fl; α-cre; R-eGFP mice, the N^d is significantly expanded anteriorly, and the C^d is significantly reduced. In many p75 fl/fl; α-cre; R-eGFP cases, the eGFP is discontinuous and has a mottled appearance, suggesting a disorganized map (arrow in [E]). L, lateral; M, medial. Scale bar, 400 μm.

Nasal RGC axons in p75 fl/fl; α-cre mice exhibit similar phenotypes as in $p75^{-/-}$ mice (Figure 8). Focal injections of DiI in nasal retina of p75 fl/fl; cre-negative mice at P8 (n = 16) reveal a projection indistinguishable from wild-type mice (Figure 8A). However, similar injections of DiI into retinas of p75 fl/fl; α-cre mice (n = 21) reveal a TZ shifted anteriorly at P8 (Figure 8B), as observed in $p75^{-/-}$ mice. Quantification of the AP position of the TZ shows a significant difference between p75 fl/fl; α-cre mice compared to wild-type littermates, confirming the anterior shift of TZs formed by p75-deficient nasal RGC axons (Figure 9A). Further, the AP position of the TZ in every p75 fl/fl; α-cre case is positioned anterior to the mean TZ position for p75 fl/fl; cre-negative mice (Figure 9B). In addition to this anterior shift of the TZ formed by p75-deficient nasal RGC axons in p75 fl/fl; α-cre mice, in a proportion of these cases the single focal DiI injection labels a dual TZ, with a TZ in the appropriate position and an ectopic TZ anterior to it (n = 3; Figure 8C).

As described above, in $p75^{+/+}$; α-cre; R-eGFP mice (n = 8; Figure 8D), the R-eGFP labeling pattern reveals the retinotopic map in the SC at a population level. As in $p75^{-/-}$ mice, we find a significant anterior shift of the N^d in the SC of p75 fl/fl; α-cre; R-eGFP mice (n = 12; Figures 8E and 8F). In addition, numerous holes are evident in the eGFP labeling pattern in the T^d of the SC, in contrast to the more uniform labeling in wild-type mice, indicative of aberrant anterior terminations of RGC axons from the eGFP-negative C^d. To quantify these mapping changes, we again measured the relative mean areas occupied by each of the three retinal projection domains in the SC. Outlines of the projection domain borders for two representative wild-type cases and a p75 fl/fl; α-cre; R-eGFP case demonstrate the anterior shift of the N^d as well as the variability in the overall projection for p75 mutant cases (Figure 9C). Overall, compared to wild-type (i.e., $p75^{+/+}$; α-cre; R-eGFP; n = 8), the N^d shows a significant increase in area in the p75 fl/fl; α-cre; R-eGFP mice (n = 12), and the C^d, which retains p75 and therefore p75-ephrin-A reverse signaling, shows a concomitant statistically significant decrease in area (Figure 9D). Because cre expression in the α-cre line is

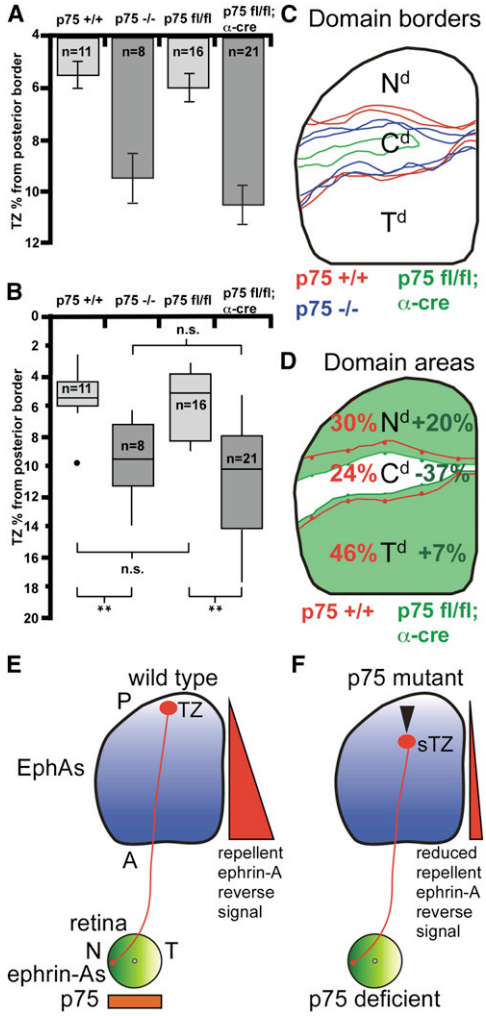

Figure 9. Quantification and Summary of Retinocollicular Shifts in p75 Mutant Mice

(A) Average position of the center of the DiI-labeled termination zones (TZs) from the posterior pole of the superior colliculus (SC) in percent of the anterior-posterior (AP) extent of the SC (error bars = SEM). There is a significant anterior shift in TZ position for $p75^{-/-}$ and p75 fl/fl; α-cre mice compared to controls. The positions of retinal injection sites between genotypes are not statistically distinct.

(B) Box plots illustrating the distributions of TZ locations. The top and bottom edges of each box are the 25th and 75th percentile, respectively. The horizontal line within each box is the median value. The vertical "whiskers" extend above and below each box to the most divergent point within three times the interquartile value. Filled circles are outliers. The distribution of TZ positions for $p75^{+/+}$ and p75 fl/fl; cre-negative are not different. However, $p75^{-/-}$ and p75 fl/fl; α-cre mice have TZ distributions significantly shifted anteriorly. Mann-Whitney U test p values for the pairs indicated: n.s., not significant; *$p < 0.01$; **$p < 0.001$.

(C) Borders of R-eGFP labeling superimposed on a dorsal view of the SC for the $p75^{+/+}$; α-cre; R-eGFP cases in Figures 6D and 8D (red). Two representative $p75^{-/-}$; α-cre; R-eGFP cases (blue; from Figures 6E and 6F) illustrate the anterior shift of the nasal domain (N^d). The p75 fl/fl; α-cre; R-eGFP case shown in Figure 8E is illustrated in green. Note the large anterior shift of the N^d and a reduced central domain (C^d).

(D) Average projection domain areas superimposed on a dorsal view of the SC. The lines indicate the average AP positions for borders of eGFP labeling for $p75^{+/+}$; α-cre; R-eGFP mice (red) and p75 fl/fl; α-cre; R-eGFP mice (green). The values for $p75^{+/+}$ cases (red) indicate the area of the SC each domain occupies, whereas the values for p75 fl/fl; α-cre cases (green) represent the percentage change from wild-type. There is a significant expansion and anterior shift of the N^d ($p < 0.01$) and a concomitant significant decrease in the C^d in p75 fl/fl; α-cre mice compared to control mice ($p < 0.01$).

(E) In wild-type mice, ephrin-As expressed in the retina (green gradient) and along retinal ganglion cell (RGC) axons interact with EphAs (blue gradient) in the SC. In addition, p75 is expressed in the retina (orange) and along RGC axons and acts as an ephrin-A signaling partner. Therefore, p75 complexes with ephrin-As along RGC axons and, upon binding EphAs in the SC, transduces a repellent ephrin-A reverse signal (red gradient) that parallels the AP gradient of EphA in the SC. Thus, nasal (N) RGC axons, expressing high levels of ephrin-As, form a TZ in posterior SC, which expresses low levels of EphAs.

(F) In p75 mutant mice, an ephrin-A signaling partner is lacking from the retina. Thus, the repellent ephrin-A reverse signal is reduced (diminished red gradient), allowing nasal RGC axons to form anteriorly shifted TZs (sTZ). The expression patterns of ephrin-As and EphAs are unchanged in p75 mutant mice. Therefore, the formation of sTZs in areas of high EphA expression is due to the loss of the ephrin-A signaling partner, p75, and the concomitant reduction in repellent ephrin-A reverse signal.

limited to nasal and temporal retina and is not evident elsewhere in the retinocollicular pathway (Marquardt et al., 2001; Baumer et al., 2002), the mapping phenotypes in the conditional and constitutive p75 knockout mice are due to the loss of p75 from RGC axons.

DISCUSSION

Reverse signaling through ephrin-As on RGC axons is implicated in the development of the retinocollicular map (Rashid et al., 2005) and in several other axonal projections (Knoll et al., 2001; Cutforth et al., 2003; Marquardt et al., 2005). However, because ephrin-As are GPI-linked proteins and lack an intracellular domain, they require a transmembrane signaling partner to initiate the intracellular pathways that carry out their functions. Here, we show that $p75^{NTR}$ is a signaling partner for ephrin-As and activates an intracellular cascade that mediates the repellent effects of ephrin-A reverse signaling on RGC axons required for their proper guidance and mapping.

We show that p75 is expressed in RGCs and that p75 protein is present in their axons in vivo at the appropriate developmental stages to mediate guidance and mapping. In addition, p75 colocalizes with ephrin-As along retinal axons and complexes with ephrin-As in caveolae. Further, this association of p75 and ephrin-A results in a functional signaling complex that when activated by EphA binding to ephrin-As leads to increased levels within caveolae of phosphorylated Fyn. Our demonstration that EphA binds ephrin-A but not p75 indicates that EphAs are not ligands per se for p75, but through its association with ephrin-As, p75 acts as coreceptor, or signaling partner, for them and is required to activate their reverse signaling pathway. We also find that the increased phosphorylation and recruitment of Fyn to caveolae is dependent upon p75, which itself is recruited to caveolae upon EphA binding ephrin-A.

Functional evidence for the p75-ephrin-A signaling complex that we describe is provided by our in vitro axon guidance assays showing that p75 is required for the repulsion of retinal axons by EphA. In contrast, p75 is not required for the repulsion of retinal

axons by ephrin-A. These data indicate that p75 is selectively required for the repellent guidance activity mediated by ephrin-A reverse signaling but is not required for the repellent guidance activity mediated by EphA forward signaling. A recent report suggested that the sensitivity of axons in peripheral nerves to the repellent activity of Sema3A is enhanced in p75 knockout mice (Ben-Zvi et al., 2007). However, we do not find evidence for an analogous role for p75 in RGC axons; that is, the lack of p75 does not lead to increased sensitivity to ephrin-A in stripe assays and that EphA forward signaling appears unaffected.

We also demonstrate that p75 is required for appropriate topographic mapping of RGC axons in the SC, by analyzing mice constitutively null for p75 or in which floxed alleles of p75 are selectively deleted from retina. In both p75 mutants, essentially all RGC axons aberrantly terminate anterior to their topographically appropriate position in the SC. This anterior shift in the terminations of p75-deficient RGC axons is the predicted outcome if the repellent activity of ephrin-A reverse signaling along the AP axis of the SC is diminished and p75 mediates this signaling (Figures 9E and 9F). In conclusion, the findings from each set of experiments in our study support the conclusion that p75 complexes with ephrin-A in RGC axon membranes and that p75 is required for the transduction of a repellent signal to RGC axons when axonally expressed ephrin-A binds EphA.

$p75^{-/-}$ mice have normal retinal morphology and numbers of RGCs (Harada et al., 2006), and we find no obvious defects in the retina or SC in either $p75^{-/-}$ mice or p75 fl/fl; α-cre mice, including the expression of ephrin-As, EphAs, and RGC markers. The α-cre mice used to delete p75 from retina in the conditional p75 knockout mice have the important feature that cre-recombinase is not expressed in the SC or anywhere in the visual pathway outside of the retina (Marquardt et al., 2001; Baumer et al., 2002). In addition, the early phases of map development appear similar in p75 mutants compared to wild-type mice. These observations, the similarity in mapping defects in the two distinct p75 mutant lines, and the consistency of the mapping defects in p75 mutant mice with results from our in vitro axon guidance assays show that the aberrant phenotypes are due to the lack of p75 in RGC axons and are not due to secondary effects.

The aberrant mapping that we observe in the p75 mutant mice is very consistent and is the predicted phenotype for a diminished action of ephrin-A reverse signaling. Our finding that the mapping defect is characterized by the formation of a relatively normal appearing TZ at an aberrant anterior position in the SC indicates that p75-deficient RGC axons are affected in a uniform manner, with essentially all RGC axons exhibiting a diminished response to ephrin-A repulsion. However, the magnitude of the anterior shift of the terminations of p75-deficient RGC axons might be viewed as subtle. It is possible that the anterior shift in terminations in p75 mutant mice is limited by the action of another signaling partner for ephrin-A partially redundant with p75, for example TROY, a transmembrane receptor that shares features with p75 (Park et al., 2005). But, even if p75 is essentially completely responsible for mediating the repellent effect of ephrin-A reverse signaling, as indicated by our findings using the protein stripe assay, we would expect the observed phenotype because other mechanisms that influence AP mapping are still intact, including competitive interactions between axons, EphA forward signaling, and "redundant" mapping mechanisms suggested to explain phenotypes in ephrin-A and EphA mutants (Frisen et al., 1998; Feldheim et al., 2000; Pfeiffenberger et al., 2006). Because essentially all p75-deficient RGC axons are affected in a uniform manner, the competitive balance between them would be retained and would act to limit the magnitude of the anterior shift of their terminations. For example, competitive interactions limit the aberrant posterior shift in the terminations of RGC axons genetically engineered to express higher levels of EphA and therefore experience higher levels of repellent EphA forward signaling (Brown et al., 2000).

The first experimental evidence for ephrin-A reverse signaling in the retinocollicular projection was reported by Rashid et al. (2005) based on the protein stripe assay and an analysis of EphA7 knockout mice. EphA7, as well as EphA3 and EphA4, is expressed in a high-to-low AP gradient in the SC, but EphA7 is not expressed in retina. In EphA7 knockout mice, a proportion of nasal RGC axons target to anterior SC rather than their appropriate TZ in posterior SC (Rashid et al., 2005). However, the proportion of nasal RGC axons that mistarget is small, and most project to their topographically correct site in posterior SC. In contrast, in p75 mutants we find that essentially all RGC axons mistarget anterior to their appropriate position in the SC, but the magnitude of the anterior shift is relatively small. Thus, in terms of appearance of the ectopic terminations, the EphA7 phenotype stands out because the subset of aberrantly projecting axons substantially mistarget, and the ectopic TZ that they form can be compared directly to the appropriate TZ that most RGCs form in the same SC. However, in terms of the proportion of axons that exhibit the aberrant phenotype, the p75 phenotype is more robust than the EphA7 phenotype.

Further, the EphA7 mutant phenotype (Rashid et al., 2005) is intriguing and perhaps unexpected because only one of several EphAs with a high-to-low AP graded expression is eliminated from the SC, and the small proportion of RGC axons affected mistarget to anterior SC that retains high EphA expression. An interpretation that explains the EphA7 mutant phenotype is that a small subset of RGCs responds differently to EphA7 than to EphA3 and EphA4. Although a basis for such a differential response has not been reported, RGCs are a heterogeneous population, with some RGC subsets comprising as little as 1% of the population (Hattar et al., 2002).

The classic function of p75 is as an NTR. BDNF, a neurotrophin ligand for the high-affinity NTR, TrkB, also binds p75 and has a general role as a growth promoter of RGC axon arbors in the retinotectal projection in *Xenopus* (Cohen-Cory and Fraser, 1995; Alsina et al., 2001). Thus, p75 may have a role as an NTR in retinocollicular development, although the TrkB mutant has been reported to have a normal retinocollicular map (Rohrer et al., 2001). Regardless, the internal consistency of our findings indicate that the phenotypes we find are due to p75 complexing with ephrin-A to mediate the repellent effect of ephrin-A reverse signaling, rather than p75 mediating growth promoting effects of BDNF. For example, in the stripe assay, wild-type retinal axons are strongly repelled by EphAs, but p75 null retinal axons are not affected, though in vitro, explants from wild-type and p75 null mice extend the same number of axons and their average

distance of extension is the same. Further, in vivo, p75-deficient RGC axons exhibit their normal, initially exuberant growth across the SC. Thus, in the absence of p75, axon repulsion due to ephrin-A reverse signaling is lost, but general features of axon growth are normal. In conclusion, p75-deficient retinal axons exhibit normal outgrowth but selectively lose their repellent response to EphAs, indicating that our findings are not due to the loss of a trophic effect of p75 but are due to the specific loss of the repellent effect of ephrin-A reverse signaling mediated by p75.

The reports of roles for ephrin-A reverse signaling in the pathfinding of spinal motor axons (Marquardt et al., 2005) and the mapping of olfactory receptor axons (Cutforth et al., 2003), which also express p75 (Carson et al., 2005; Domeniconi et al., 2007) suggest the possibility that p75 acts as a signaling partner with ephrin-As in other developing projection systems. In addition, Fyn, which is a prominent component of the p75-ephrin-A signaling pathway, is also an important contributor to the signaling pathways of other guidance molecules, including netrin/DCC and sema3A (Sasaki et al., 2002; Liu et al., 2004; Meriane et al., 2004). Thus, it is likely that p75 acts broadly as a partner for ephrin-A reverse signaling and potentially other families of axon guidance molecules and their signaling pathways, suggesting that both p75 and Fyn are involved in integrating multiple signaling pathways to provide coherent guidance information.

EXPERIMENTAL PROCEDURES

Immunohistochemistry

Anesthetized mice were perfused with 4% paraformaldehyde (PF), dissected, and cryoprotected in 30% sucrose. Cryostat sections (20 μm) were processed with antibodies and receptor affinity probes from R&D Systems (anti-ephrin-A2, AF603; anti-ephrin-A5, AF3743; ephrin-A5-Fc, 374-EA) and Santa Cruz (anti-p75, sc-6188; Brn3.2, sc-6026). Some retinal sections were labeled with anti-GFP antibodies (Molecular Probes, A11122). Retinal axons and 293 cells grown in vitro were fixed with 4% PF in PBS for 10–15 min, washed, and processed with the reagents above as well anti-Fc antibody (Jackson Immuno, 309-166-008) and EphA7-Fc (R&D Systems, 608-A7).

Immunoprecipitation

For Figure 2A, mouse retinas were lysed in RIPA buffer (150 mM NaCl, 1% NP-40, 0.5% DOC, 0.1% SDS, 50 mM Tris [pH 8.0]). Lysates were immunoprecipitated with anti-p75 intracellular domain antibody (Buster, a gift from Philip A. Barker, McGill University) or anti-ephrin-A2 antibody (R&D Systems, AF603). Immunoprecipitations were performed using ExactaCruz F and C kits (Santa Cruz, sc-45043 and sc-45040) to decrease IgG bands. Samples were analyzed using SDS-PAGE and western blots. For detection of p75 and ephrin-A2, anti-p75 antibody (Buster) and anti-ephrin-A2 antibody (Santa Cruz, L-20, sc-912) were used, respectively. For Figure 2B, PC12 cells were transfected with linearized V5-tagged ephrin-A2 construct by TransFectin lipid reagent (Biorad, 170-3352) and selected by puromycin (2 μg/ml) for at least 14 days. Colonies were picked and characterized by immunocytochemistry and western blots. PC12 and stably transfected V5-ephrin-A2/PC12 cells were lysed in RIPA buffer and immunoprecipitated with either anti-p75 (Buster) or anti-V5 antibody (Invitrogen, R960-25). For detection of p75 and V5-ephrin-A2, anti-p75 antibody (Buster) and anti-V5 antibody (Invitrogen) were used. For Figure 2C, 293T cells were transiently transfected with cMyc-tagged p75 and/or V5-tagged ephrin-A5 or ephrin-A2 constructs by TransFectin. Cells were lysed in RIPA buffer and immunoprecipitated with either anti-cMyc antibody (Santa Cruz, 9E10, sc-40) or anti-V5 antibody (Invitrogen). For detection of p75 and V5-ephrin-A2/5, anti-p75 antibody (Buster) and anti-V5 antibody (Invitrogen) were used.

Isolation of Caveolae

Stably transfected 293 cell lines (ephrin-A2, p75, and ephrin-A2/p75) were made by transfecting with linearized V5-tagged ephrin-A2 and/or cMyc tagged p75 constructs using TransFectin™ and selected by puromycin (2 μg/ml) and/or G418 (400 μg/ml) for at least 14 days. Colonies were picked and characterized by immunocytochemistry and western blots. Detergent-resistant membrane fractions containing caveolae were prepared by modifying a procedure originally described by Higuchi et al. (2003). Cells were grown to 90% confluence and serum-starved for 18 hr before treatment. Cells were treated with either human-Fc (R&D systems, 110-HG, 2 μg/ml) or EphA7-Fc (R&D Systems, 608-A7, 2 μg/ml) for 10 min at 37°C, then lysed on ice with 1 ml of 0.5% Brij-58 (Sigma) in buffer containing 10 mM Tris (pH 7.5), 1 mM EDTA, 150 mM NaCl, 10% glycerol, phosphatase inhibitor cocktail I and II, and protease inhibitor cocktail (Sigma). Lysed cells were scraped from plates into individual tubes and kept on ice for 30 min. Lysates were adjusted to 40% sucrose, 2 ml of the mixture was placed in the bottom of an SW41Ti ultracentrifuge tube (Beckman), and overlaid with 8 ml of 30% sucrose and 2 ml of distilled water. All steps from lysis to centrifugation were performed at 4°C. After centrifugation (16 hr, 35,000 rpm, 4°C), 1 ml fractions were collected from the top to the bottom (numbered from 1 to 12). The proteins in each fraction were precipitated for concentration and sucrose removal. Briefly, 600 μl methanol was added to 150 μl of each fraction. After thorough mixing, 150 μl of chloroform was added. After vortexing, 450 μl of water was added, vortexed again, and centrifuged for 5 min at full speed in a microcentrifuge. The upper aqueous layer was discarded, 650 μl of methanol added, and each tube was inverted three times. After 5 min at full speed in a microcentrifuge, all liquid was removed and the pellets were air-dried. Equal volume of Laemmli's sample buffer (30 μl) was added, samples were heated at 100°C for 5 min, and prepared for SDS-PAGE and western blot analyses. For detection of tyrosine phosphorylation, Fyn, p75, V5-tagged ephrin-A2, flotillin-1 and GM1, phosphotyrosine-specific antibody 4G10 (a gift from Tony Hunter, Salk Institute), anti-Fyn antibody (Santa Cruz, sc-16), anti-p75 intracellular domain antibody (Buster), anti-V5 antibody (Invitrogen, R960-25), anti-flotillin-1 antibody (BD Transduction Laboratories, 610820) and CTX-HRP (Invitrogen, C34780) were used.

Mice

p75 null mutants were described previously (Lee et al., 1992). To generate p75 conditional mutants, two LoxP sites were introduced into the p75 locus to flank exon 3 through homologous recombination in embryonic stem cells (Z. Chen, T.-C.S., N. Harada, W. Lin, and K.-F.L., unpublished data). p75 conditional mutants were crossed with α-cre transgenic mice (Marquardt et al., 2001) generously provided by Peter Gruss. In some cases the ROSA-GAP43-eGFP allele was also present (mice generously provided by Martyn Goulding; Sapir et al., 2004). Animal protocols were approved by the Salk Institute Animal Care and Use Committee and conform to NIH guidelines.

Stripe Assays

Retinas from P0–P2 mice were dissected, flattened onto a nitrocellulose filter, and cut into strips 150–400 μm wide. Strips were plated, RGC side down, onto glass coverslips or plastic dishes coated with alternating stripes of human-Fc or EphA7-Fc and human-Fc or ephrin-A5-Fc and human-Fc (R&D Systems 110-HG; 15–30 μg/ml) and laminin. Stripes were made essentially as described (Hornberger et al., 1999; Rashid et al., 2005). After 2–4 days, explants were stained with carboxyfluorescein diacetate, succinimidyl ester (fluorescent vital dye; Molecular Probes), examined, photographed, and scored independently by two investigators blind to experimental condition, lane content, and genotype of the explant source. A score of zero indicates no discernible choice; one indicates any detectable bias; two indicates a clear bias; three indicates a strong and significant choice for a significant majority of axons; four indicates an essentially complete choice for one lane. Pixel values were determined by thresholding each grayscale photo using Adobe Photoshop until pixels representing axons were white and background was black. Pixels clearly representing debris were converted to background. Pixels were counted in each lane and normalized for lane width. The modified Sholl intersection analysis was performed by delineating the edge of each explant and points 100 μm, 300 μm, 600 μm, 900 μm away. Blind to genotype, lane condition, and lane position, all intersections between axons and the transposed

explant outlines were digitally marked. With all intersections marked, lane boundaries were overlaid, and the position of each intersection point was assigned to a lane and normalized for lane width. The coefficient of choice is defined as the total pixels representing axons or intersections on control lanes minus that on the second human-Fc lane, or the EphA7-Fc or ephrin-A5-Fc lanes, divided by total pixels or intersections. A coefficient of one indicates an absolute choice for the control lane, a coefficient of zero indicates no choice, and a negative coefficient of choice indicates a choice for the second human-Fc or EphA7-Fc or ephrin-A5-Fc lane.

Axon Tracing and Analysis

Focal injections of the lipophilic, fluorescent axon tracer DiI (Molecular Probes) were made via pressure injection through a glass micropipette tip into the retina and allowed to transport for 16–24 hr. Mice were perfused, dissected, and axon labeling photographed. Some midbrains were sectioned on a vibratome at 100–200 μm. The focal nature and fidelity of all injections was determined by retinal flat-mounts examined under fluorescence. All labeled axons originated from a single focal location in every case reported.

Analyses of TZ position, DiI injection location, and eGFP domains in the SC were performed on digital images in Adobe Photoshop or NIH ImageJ software and analyzed with Excel or KaleidaGraph software. The center of the DiI injection and TZ were used for the analyses and determined to be the center of a circumscribed circle. For the analysis of eGFP-labeled projection domains, the SC was divided into ten equal segments along the LM axis. The anterior and posterior borders of the central domain were determined in each segment by thresholding at three times the average pixel value of an arbitrarily selected area within the central domain of that segment. Segments were combined, and pixel values counted in the three defined domains. Values for domain sizes are normalized. Total SC area is not statistically different between genotypes.

ACKNOWLEDGMENTS

We thank Sourav Ghosh and Tony Hunter for their expertise and help with preliminary immunoprecipitations, Sam Pfaff for comments on the manuscript, Berta Higgins and Haydee Gutierrez for technical assistance, Peter Gruss for the α-Cre mice and Martyn Goulding for the ROSA-GAP43-eGFP reporter mice. Supported by National Eye Institute grant R01 EY 07025 (D.O'L.) and the Joseph Alexander Foundation.

Accepted: July 21, 2008
Published: September 10, 2008

REFERENCES

Alsina, B., Vu, T., and Cohen-Cory, S. (2001). Visualizing synapse formation in arborizing optic axons in vivo: dynamics and modulation by BDNF. Nat. Neurosci. *4*, 1093–1101.

Barker, P.A. (2004). p75NTR is positively promiscuous: novel partners and new insights. Neuron *42*, 529–533.

Baumer, N., Marquardt, T., Stoykova, A., Ashery-Padan, R., Chowdhury, K., and Gruss, P. (2002). Pax6 is required for establishing naso-temporal and dorsal characteristics of the optic vesicle. Development *129*, 4535–4545.

Ben-Zvi, A., Ben-Gigi, L., Klein, H., and Behar, O. (2007). Modulation of Semaphorin3A activity by p75 neurotrophin receptor influences peripheral axon patterning. J. Neurosci. *27*, 13000–13011.

Brown, A., Yates, P.A., Burrola, P., Ortuño, D., Vaidya, A., Jessell, T.M., Pfaff, S.L., O'Leary, D.D.M., and Lemke, G. (2000). Topographic mapping from the retina to the midbrain is controlled by relative but not absolute levels of EphA receptor signaling. Cell *7*, 77–88.

Carson, C., Saleh, M., Fung, F.W., Nicholson, D.W., and Roskams, A.J. (2005). Axonal dynactin p150Glued transports caspase-8 to drive retrograde olfactory receptor neuron apoptosis. J. Neurosci. *25*, 6092–6104.

Chao, M.V. (2003). Neurotrophins and their receptors: a convergence point for many signaling pathways. Nat. Rev. Neurosci. *4*, 299–309.

Cohen-Cory, S., and Fraser, S.E. (1995). Effects of brain-derived neurotrophic factor on optic axon branching and remodelling in vivo. Nature *378*, 192–196.

Cowan, C.A., and Henkemeyer, M. (2002). Ephrins in reverse, park and drive. Trends Cell Biol. *12*, 339–346.

Cutforth, T., Moring, L., Mendelsohn, M., Nemes, A., Shah, N.M., Kim, M.M., Frisen, J., and Axel, R. (2003). Axonal ephrin-As and odorant receptors. Coordinate determination of the olfactory sensory map. Cell *114*, 311–322.

Davy, A., and Robbins, S.M. (2000). Ephrin-A5 modulates cell adhesion and morphology in an integrin-dependent manner. EMBO J. *19*, 5396–5405.

Davy, A., Gale, N.W., Murray, E.W., Klinghoffer, R.A., Soriano, P., Feuerstein, C., and Robbins, S.M. (1999). Compartmentalized signaling by GPI-anchored ephrin-A5 requires the Fyn tyrosine kinase to regulate cellular adhesion. Genes Dev. *13*, 3125–3135.

Domeniconi, M., Hempstead, B.L., and Chao, M.V. (2007). Pro-NGF secreted by astrocytes promotes motor neuron cell death. Mol. Cell. Neurosci. *734*, 271–279.

Feldheim, D.A., Vanderhaeghen, P., Hansen, M.J., Frisén, J., Lu, Q., Barbacid, M., and Flanagan, J.G. (1998). Topographic guidance labels in a sensory projection to the forebrain. Neuron *21*, 1303–1313.

Feldheim, D.A., Kim, Y.I., Bergemann, A.D., Frisén, J., Barbacid, M., and Flanagan, J.G. (2000). Genetic analysis of ephrin-A2 and ephrin-A5 shows their requirement in multiple aspects of retinocollicular mapping. Neuron *25*, 563–574.

Flanagan, J.G. (2006). Neural map specification by gradients. Curr. Opin. Neurobiol. *16*, 59–66.

Frisen, J., Yates, P.A., McLaughlin, T., Friedman, G.C., O'Leary, D.D.M., and Barbacid, M. (1998). Ephrin-A5 (AL-1/RAGS) is essential for proper retinal axon guidance and topographic mapping in the mammalian visual system. Neuron *20*, 235–243.

Gale, N.W., Holland, S.J., Valenzuela, D.M., Flenniken, A., Pan, L., Ryan, T.E., Henkemeyer, M., Strebhardt, K., Hirai, H., Wilkinson, D.G., et al. (1996). Eph receptors and ligands comprise two major specificity subclasses and are reciprocally compartmentalized during embryogenesis. Neuron *17*, 9–19.

Grunwald, I.C., and Klein, R. (2002). Axon guidance: receptor complexes and signaling mechanisms. Curr. Opin. Neurobiol. *12*, 250–259.

Harada, C., Harada, T., Nakamura, K., Sakai, Y., Tanaka, K., and Parada, L.F. (2006). Effect of p75NTR on the regulation of naturally occurring cell death and retinal ganglion cell number in the mouse eye. Dev. Biol. *290*, 57–65.

Hattar, S., Liao, H.W., Takao, M., Berson, D.M., and Yau, K.W. (2002). Melanopsin-containing retinal ganglion cells: architecture, projections, and intrinsic photosensitivity. Science *295*, 1065–1070.

Higuchi, H., Yamashita, T., Yoshikawa, H., and Tohyama, M. (2003). PKA phosphorylates the p75 receptor and regulates its localization to lipid rafts. EMBO J. *22*, 1790–1800.

Hornberger, M.R., Dutting, D., Ciossek, T., Yamada, T., Handwerker, C., Lang, S., Weth, F., Huf, J., Wessel, R., Logan, C., et al. (1999). Modulation of EphA receptor function by coexpressed ephrinA ligands on retinal ganglion cell axons. Neuron *22*, 731–742.

Huai, J., and Drescher, U. (2001). An ephrin-A-dependent signaling pathway controls integrin function and is linked to the tyrosine phosphorylation of a 120-kDa protein. J. Biol. Chem. *276*, 6689–6694.

Huang, E.J., and Reichardt, L.F. (2003). Trk receptors: roles in neuronal signal transduction. Annu. Rev. Biochem. *72*, 609–642.

Huber, A.B., Kolodkin, A.L., Ginty, D.D., and Cloutier, J.F. (2003). Signaling at the growth cone: ligand-receptor complexes and the control of axon growth and guidance. Annu. Rev. Neurosci. *26*, 509–563.

Jing, S., Wen, D., Yu, Y., Holst, P.L., Luo, Y., Fang, M., Tamir, R., Antonio, L., Hu, Z., Cupples, R., et al. (1996). GDNF-induced activation of the ret protein tyrosine kinase is mediated by GDNFR-alpha, a novel receptor for GDNF. Cell *85*, 1113–1124.

Knoll, B., Zarbalis, K., Wurst, W., and Drescher, U. (2001). A role for the EphA family in the topographic targeting of vomeronasal axons. Development *128*, 895–906.

Kullander, K., and Klein, R. (2002). Mechanisms and functions of Eph and ephrin signalling. Nat. Rev. Mol. Cell Biol. *3*, 475–486.

Lee, K.F., Li, E., Huber, L.J., Landis, S.C., Sharpe, A.H., Chao, M.V., and Jaenisch, R. (1992). Targeted mutation of the gene encoding the low affinity NGF receptor p75 leads to deficits in the peripheral sensory nervous system. Cell *69*, 737–749.

Liu, G., Beggs, H., Jürgensen, C., Park, H.T., Tang, H., Gorski, J., Jones, K.R., Reichardt, L.F., Wu, J., and Rao, Y. (2004). Netrin requires focal adhesion kinase and Src family kinases for axon outgrowth and attraction. Nat. Neurosci. *7*, 1222–1232.

Marquardt, T., Ashery-Padan, R., Andrejewski, N., Scardigli, R., Guillemot, F., and Gruss, P. (2001). Pax6 is required for the multipotent state of retinal progenitor cells. Cell *105*, 43–55.

Marquardt, T., Shirasaki, R., Ghosh, S., Andrews, S.E., Carter, N., Hunter, T., and Pfaff, S.L. (2005). Coexpressed EphA receptors and ephrin-A ligands mediate opposing actions on growth cone navigation from distinct membrane domains. Cell *121*, 127–139.

McLaughlin, T., and O'Leary, D.D.M. (2005). Molecular gradients and development of retinotopic maps. Annu. Rev. Neurosci. *28*, 327–355.

Meriane, M., Tcherkezian, J., Webber, C.A., Danek, E.I., Triki, I., McFarlane, S., Bloch-Gallego, E., and Lamarche-Vane, N. (2004). Phosphorylation of DCC by Fyn mediates Netrin-1 signaling in growth cone guidance. J. Cell Biol. *167*, 687–698.

Murai, K.K., and Pasquale, E.B. (2003). 'Eph'ective signaling: forward, reverse and crosstalk. J. Cell Sci. *15*, 2823–2832.

Park, J.B., Yiu, G., Kaneko, S., Wang, J., Chang, J., He, X.L., Garcia, K.C., and He, Z. (2005). A TNF receptor family member, TROY, is a coreceptor with Nogo receptor in mediating the inhibitory activity of myelin inhibitors. Neuron *45*, 345–351.

Parton, R.G. (1994). Ultrastructural localization of gangliosides; GM1 is concentrated in caveolae. J. Histochem. Cytochem. *42*, 155–166.

Peles, E., Nativ, M., Lustig, M., Grumet, M., Schilling, J., Martinez, R., Plowman, G.D., and Schlessinger, J. (1997). Identification of a novel contactin-associated transmembrane receptor with multiple domains implicated in protein-protein interactions. EMBO J. *16*, 978–988.

Pfeiffenberger, C., Yamada, J., and Feldheim, D.A. (2006). Ephrin-As and patterned retinal activity act together in the development of topographic maps in the primary visual system. J. Neurosci. *26*, 12873–12884.

Rashid, T., Upton, A.L., Blentic, A., Ciossek, T., Knoll, B., Thompson, I.D., and Drescher, U. (2005). Opposing gradients of ephrin-As and EphA7 in the superior colliculus are essential for topographic mapping in the mammalian visual system. Neuron *47*, 57–69.

Rohrer, B., LaVail, M.M., Jones, K.R., and Reichardt, L.F. (2001). Neurotrophin receptor TrkB activation is not required for the postnatal survival of retinal ganglion cells in vivo. Exp. Neurol. *172*, 81–91.

Sapir, T., Geiman, E.J., Wang, Z., Velasquez, T., Mitsui, S., Yoshihara, Y., Frank, E., Alvarez, F.J., and Goulding, M. (2004). Pax6 and engrailed 1 regulate two distinct aspects of renshaw cell development. J. Neurosci. *24*, 1255–1264.

Sasaki, Y., Cheng, C., Uchida, Y., Nakajima, O., Ohshima, T., Yagi, T., Taniguchi, M., Nakayama, T., Kishida, R., Kudo, Y., et al. (2002). Fyn and Cdk5 mediate semaphorin-3A signaling, which is involved in regulation of dendrite orientation in cerebral cortex. Neuron *35*, 907–920.

Sholl, D.A. (1953). Dendritic organization in the neurons of the visual and motor cortices of the cat. J. Anat. *87*, 387–406.

Simons, K., and Toomre, D. (2000). Lipid rafts and signal transduction. Nat. Rev. Mol. Cell Biol. *1*, 31–39.

Slaughter, N., Laux, I., Tu, X., Whitelegge, J., Zhu, X., Effros, R., Bickel, P., and Nela, A. (2003). The flotillins are integral membrane proteins in lipid rafts that contain TCR-associated signaling components: implications for T-cell activation. Clin. Immunol. *108*, 138–151.

Tessier-Lavigne, M., and Goodman, C.S. (1996). The molecular biology of axon guidance. Science *274*, 1123–1133.

Trupp, M., Raynoschek, C., Belluardo, N., and Ibanez, C.F. (1998). Multiple GPI-anchored receptors control GDNF-dependent and independent activation of the c-Ret receptor tyrosine kinase. Mol. Cell. Neurosci. *11*, 47–63.

Walter, J., Kern-Veits, B., Huf, J., Stolze, B., and Bonhoeffer, F. (1987). Recognition of position-specific properties of tectal cell membranes by retinal axons in vitro. Development *101*, 685–696.

Xiang, M., Zhou, L., Peng, Y.W., Eddy, R.L., Shows, T.B., and Nathans, J. (1993). Brn-3b: a POU domain gene expressed in a subset of retinal ganglion cells. Neuron *11*, 689–701.

Yates, P.A., Holub, A.D., McLaughlin, T., Sejnowski, T.J., and O'Leary, D.D.M. (2004). Computational modeling of retinotopic map development to define contributions of EphA-ephrinA gradients, axon-axon interactions, and patterned activity. J. Neurobiol. *59*, 95–113.